Burst synchronization transitions in a neuronal network of subnetworks

Xiaojuan Sun,[1,a)] Jinzhi Lei,[1,b)] Matjaž Perc,[2,c)] Jürgen Kurths,[3,d)] and Guanrong Chen[4,e)]
[1]*Zhou Pei-Yuan Center for Applied Mathematics, Tsinghua Univeristy, Beijing 100084, People's Republic of China*
[2]*Department of Physics, Faculty of Natural Sciences and Mathematics, University of Maribor, Koroška cesta 160, SI-2000 Maribor, Slovenia*
[3]*Potsdam Institute for Climate Impact Research, 14412 Potsdam, Germany and Institute of Physics, Humboldt University Berlin, 12489 Berlin, Germany*
[4]*Department of Electronic Engineering, City University of Hong Kong, Hong Kong SAR, People's Republic of China*

(Received 15 November 2010; accepted 2 February 2011; published online 29 March 2011)

In this paper, the transitions of burst synchronization are explored in a neuronal network consisting of subnetworks. The studied network is composed of electrically coupled bursting Hindmarsh–Rose neurons. Numerical results show that two types of burst synchronization transitions can be induced not only by the variations of intra- and intercoupling strengths but also by changing the probability of random links between different subnetworks and the number of subnetworks. Furthermore, we find that the underlying mechanisms for these two bursting synchronization transitions are different: one is due to the change of spike numbers per burst, while the other is caused by the change of the bursting type. Considering that changes in the coupling strengths and neuronal connections are closely interlaced with brain plasticity, the presented results could have important implications for the role of the brain plasticity in some functional behavior that are associated with synchronization. © *2011 American Institute of Physics*. [doi:10.1063/1.3559136]

Synchronization in complex networks has been discussed extensively in the past years. In nature, many complex networks (e.g., biological networks) are modular, i.e., composed of certain subgraphs with differential internal and external connectivity. And some interesting results about synchronization in modular networks have been reported recently. Moreover, it is known that synchronization of complex dynamical networks results from the interplay between the intrinsic properties of individual dynamical system and the network topology. Therefore, modeling each node by a neuronal system and discussing synchronization in modular networks can extend the works on the understanding of dynamics, especially synchronization, in such networks. On the other hand, synchronous activities are revealed to have close relationships with pathological brain states and cognitive functions. And the cortical network is a very complex network with hierarchy and modular (or clustered) structures. Thus, studying neuronal dynamics of a network of subnetworks (modular network) is also very meaningful to neuroscientists. In this paper, we study synchronization of bursting neurons in a modular neuronal network, which contains several subnetworks. By means of numerical simulations, we find that burst synchronization transitions can be induced by several factors, such as the intra- and intercoupling strengths, the number of links between different subnetworks, as well as the number of subnetworks. As is well known, plasticity is an important property of the brain, and changes in the coupling strength and the number of connections per neuron are two factors that affect this property. It is therefore suggested that the presented results could facilitate our understanding not only of synchronization in modular networks but also of plasticity and its impact on synchronization in neuronal networks.

I. INTRODUCTION

Synchronization phenomena are ubiquitous in nature. Insightful findings regarding the synchronization in complex networks were reported extensively in the past years[1–8] and comprehensively reviewed in Ref. 9 recently. Previous works have found that small-world,[1,2] scale-free,[3] and weighted networks[4,5] are generally more synchronizable than regular networks. In nature, many complex networks are modular, i.e., composed of certain subgraphs with differential internal and external connectivity. More recently, synchronization in complex modular (or clustered) networks has been investigated.[10–14] For example, synchronization of a clustered network with random subnetworks can be suppressed if extra links are added improperly.[11] For a clustered network with regular subnetworks, it has been revealed that the network exhibits strong and weak synchronizability (complete synchronization) in an alternating manner.[13]

As is well known, synchronization of complex dynamical network systems results from the interplay between the intrinsic properties of individual dynamical system and the

[a)]Author to whom correspondence should be addressed. Electronic mail: sunxiaojuan.bj@gmail.com.
[b)]Electronic mail: jinzhi.lei@gmail.com.
[c)]Electronic mail: matjaz.perc@uni-mb.si.
[d)]Electronic mail: kurths@pik-potsdam.de.
[e)]Electronic mail: eegchen@cityu.edu.hk.

network topology. Each property may play an important role in shaping the emergence of synchronous behaviors. Therefore, modeling each node by a neuronal system and discussing synchronization in modular networks can extend the interest of the work on the understanding of dynamics in such networks.

Additionally, synchronous activity has been also observed in neuronal systems[15–17] and reported to be associated not only with pathological brain states[18–20] but also with various cognitive functions.[21–23] Moreover, the cortical network is revealed to be a hierarchical and modular (or clustered) network with a complex connectivity.[24–26] In order to better understand the brain, it is necessary to study neuronal dynamics of networks at a mesoscopic level (if we classify an individual network of interacting neurons as at the microscopic level). Thus, investigating synchronization phenomena of neuronal systems in modular networks is also very meaningful to neuroscientists.

As mentioned above, synchronization has been widely observed in neuronal systems. However, the underlying mechanisms for the occurrence of synchronization and the effects of many (internal and external) factors on synchronization in neuronal systems are far from being fully understood. It is phenomenal that many studies reported in the focus on synchronization phenomena of neuronal systems in the last decade,[27–37] among which most are about synchronization of spiking neurons. As the other basic firing activity, bursting is reported to have many functional implications, see the Ref. 38 for a detailed review. Therefore, more attention should also be paid on synchronization of bursting neurons.

Synchronization of bursting neurons includes the synchrony on the spiking time scale (spike synchronization) and synchrony on the bursting time scale (burst synchronization). Recently, some researchers have turned their attention to study synchronization of bursting neurons and have obtained interesting results.[39–42] As revealed by Ref. 40, burst synchronization could be a precursor to spike synchronization. Moreover, it has been found that burst synchronization of neuronal systems may be influenced strongly by many factors, such as coupling strengths and types,[43–45] time delays,[46,47] and noise.[48–50] Additionally, it has been reported that synchronization among chaotically bursting neurons could lead to the onset of regular bursting.[51]

More recently, a seemingly more interesting phenomena—synchronization transition—has been reported in some neuronal networks.[52–56] It has been found that coupling strength and time delays could induce synchronization transitions not only in electrically coupled neuronal networks[52,53] but also in chemically coupled ones.[54–56] To our knowledge, there are still no corresponding works on studying synchronization transition of bursting neurons in modular networks. Therefore, in this paper, we will take a first step on this topic by studying burst synchronization transition in a network of subnetworks, with each subnetwork being an independent one consisting of a group of electrically coupled bursting Hindmarsh–Rose neurons.[57]

In the following section, we introduce a mathematical model of the system. Then, we present our numerical results of the studied neuronal network. Finally, we give a short discussion and draw some conclusions.

II. MODEL AND MEASUREMENT

A. Model

As mentioned in the Introduction, we will study burst synchronization in a network of subnetworks. The structure of a network of subnetworks can be generated in the following way. We assume that there are M subnetworks, with each subnetwork consisting of n_I $(I=1,\ldots,M)$ nodes; we randomly choose some pairs of nodes from the Ith and Jth subnetworks ($I=1,\ldots,M$, $J=1,\ldots,M$, and $I\neq J$) and then add links between them. By doing so, a network of subnetworks is generated. The subnetworks could be regular, small-world, or scale-free networks. Moreover, they could have similar or dissimilar network properties and the same number of nodes or not. Clustered networks studied in Refs. 11 and 13 are two typical samples of the network of subnetworks.

In this paper, we consider that each subnetwork contains equal number of nodes, i.e., $n_I=n$ is independent of the index I. And nodes in each subnetwork are arranged on a ring, with each node connected to its $2k$ nearest neighbors. Especially, we assume that M subnetworks are also arranged on a ring, and neurons in each subnetwork just connect to the neurons from its two nearest subnetworks. The interconnections between different subnetworks exist randomly with the probability p. In our case, the parameter p represents the fraction of total links in the network devoted to the connections between different subnetworks. And if the network size N is fixed, then the number of links between different subnetworks can be expressed as $(p/M)N^2$. Thus, changes of parameter p and M could induce changes of the number of interlinks of the network.

An example of the considered network topology is shown in Fig. 1. In Fig. 1, which serves illustrative purposes, there are three subnetworks, each consisting of 25 neurons. Neurons inside each subnetwork have six nearest neighbors, and the number of links between neurons from different subnetwork is seven (here $p\approx 0.004$). In this paper, N and k are taken as 240 and 5, respectively.

The Hindmarsh–Rose (HR) model was originally introduced to give a bursting type with long interspike intervals of real neurons.[57] In this paper, we use it as the local model for each node in the studied neuronal network of networks. The equations of the neuronal network are as follows:

$$\begin{aligned}\dot{x}_{I,i} &= y_{I,i} - ax_{I,i}^3 + bx_{I,i}^2 - z_{I,i} + I_{\text{ext}} + \epsilon_{\text{intra}} \\ &\quad \times \sum_j A_I(i,j)(x_{I,j} - x_{I,i}) \\ &\quad + \epsilon_{\text{inter}} \sum_J \sum_j B_{I,J}(i,j)(x_{J,j} - x_{I,i}), \qquad (1) \\ \dot{y}_{I,i} &= c - dx_{I,i}^2 - y_{I,i}, \\ \dot{z}_{I,i} &= r[s(x_{I,i} - x_0) - z_{I,i}],\end{aligned}$$

where the variable x represents the membrane action potential, y represents the fast current, like currents of Na^+ or K^+,

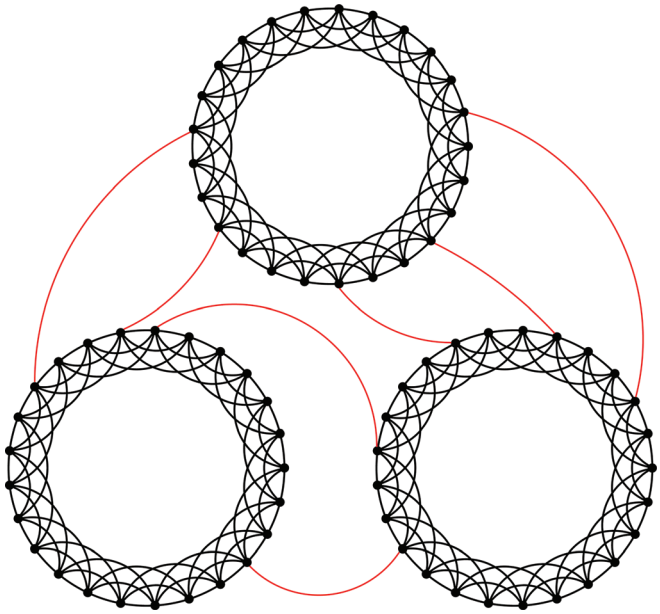

FIG. 1. (Color online) Schematic presentation of the considered network architecture. The whole network consists of $M = 3$ subnetworks, each containing $n_I = 25$ neurons. Within each subnetwork, every neuron is connected to its six nearest neighbors, and there are seven connections amongst neurons from different subnetworks.

and z associates with the slow current, e.g., a current of Ca^{2+}. The system parameters a, b, c, d, r, s, x_0 are taken as $a=1.0$, $b=3.0$, $c=1.0$, $d=5.0$, $r=0.006$, $s=4.0$, $x_0 = -1.6$, and the external current I_{ext} is taken as $I_{\text{ext}} = 3.0125$, where an isolated neuron produces chaotic bursting activity. Here, we should clarify that the chaotic bursting state can be suppressed by coupling items of the network (cf. Fig. 12). ϵ_{intra} is the coupling strength among neurons inside each subnetwork, while ϵ_{inter} is the coupling strength of neurons between different subnetworks. The subscript pairs (I,i) represent the ith neuron in the Ith subnetwork, $i=1,\ldots,n$ and $I=1,\ldots,M$. The matrix $A_I=(A_I(i,j))$ is an intraconnectivity matrix for the Ith subnetwork: $A_I(i,j)=A_I(j,i)=1$ if neuron i is connected to neuron j inside the Ith subnetwork, $A_I(i,j)=A_I(j,i)=0$ otherwise, and $A_I(i,i)=0$. The matrix $B_{I,J}=B_{I,J}(i,j)$ is also a connectivity matrix, but this matrix represents the interconnections between neurons which belong to different subnetworks: $B_{I,J}(i,j)=B_{I,J}(i,j) = 1$ if the ith neuron in the Ith subnetwork is connected to the jth neuron in the Jth subnetwork, $B_{I,J}(i,j)=B_{I,J}(i,j) = 0$ otherwise. The numerical integrations of the model, Eq. (1), are performed by using Eular integration with a time step size 0.001 ms. The results shown below are averaged over ten independent realizations of the network for any given values of p.

B. Measurement

In order to quantitatively characterize the synchronization degree of the bursting neurons, we calculate the order parameter R which is defined as[58]

$$R=\frac{1}{N}\left|\sum_{j=1}^{N}\exp[i\phi_j(t)]\right|, \tag{2}$$

where $\phi_j(t)$ is the burst phase for the jth neuron at the time t and can be presented as[41]

$$\phi_j(t)=2\pi\frac{t-T_{j,k}}{T_{j,k+1}-T_{j,k}}, \quad T_{j,k}\le t\le T_{j,k+1}, \tag{3}$$

where $T_{j,k}$ is the moment at which the kth burst of the jth neuron starts, $j = 1, ..., N$. R is zero for weak correlation and tends to unity for a full burst synchronization state. Larger R means higher degree of burst synchronization of the neuronal network.

III. RESULTS

A. Burst synchronization transition in a network of subnetworks with $M = 2$

For simplicity, we first study burst synchronization transition in a network with two subnetworks, namely, $M=2$. We will take the intercoupling strength ϵ_{inter}, the intracoupling strength ϵ_{intra}, and the probability p with which the random links between different subnetworks exist, as control parameters in the following.

First, we set $\epsilon_{\text{inter}}=0.008$ and $\epsilon_{\text{intra}}=0.0052$ such that the clustered networks are burst synchronized when $p=0$ (the corresponding spatiotemporal pattern is not shown here); we take the probability p as control parameter. Figure 2 shows the spatiotemporal patterns observed on the network for five different probabilities p. With the increasing of p, three burst synchronized patterns can be observed, as shown in Figs. 2(a), 2(c), and 2(e). The spatiotemporal patterns shown in Figs. 2(b) and 2(d) are transition patterns between two burst synchronization states Figs. 2(a) and 2(c), and 2(c) and 2(e), respectively. Thus, for fixed ϵ_{inter} and ϵ_{intra}, the random link probability p between subnetworks induces burst synchronization transitions in a neuronal network, which has two subnetworks.

Variation of the order parameter R with respect to the probability p is plotted in Fig. 3, where ϵ_{inter} and ϵ_{intra} are

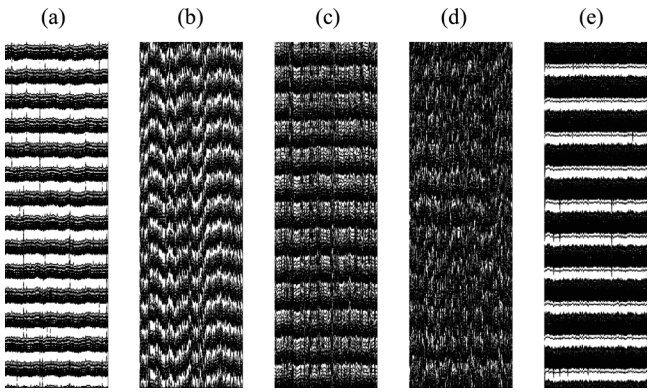

FIG. 2. Two burst synchronization transitions are induced by the random link probability p. The spatiotemporal patterns shown in (a) $p=0.015$, (c) $p=0.065$, and (e) $p=0.17$ are burst synchronized patterns, while the spatiotemporal patterns shown in (b) $p=0.045$ and (d) $p=0.085$ are the transition ones. Here $N=240, M=2$, and $\epsilon_{\text{inter}}=0.008, \epsilon_{\text{intra}}=0.0052$. The vertical and horizontal of the spatiotemporal patterns indicates time and neuron index, respectively. The color profile is linear, black depicting $x_i(t)=1.5$ and white $x_i(t)=-1.6, i=1,\ldots,N$.

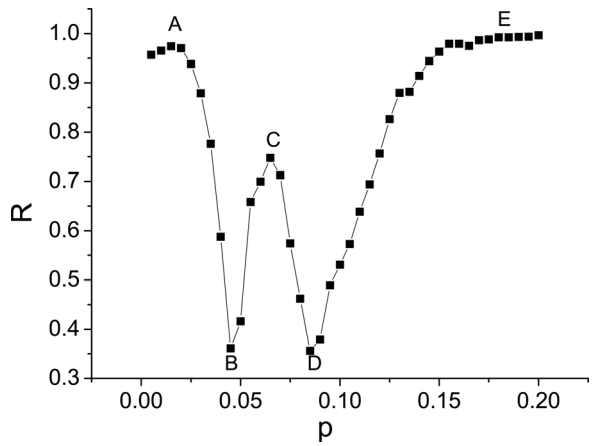

FIG. 3. Variation of the order parameter R with respect to p for $\epsilon_{\text{inter}}=0.008$ and $\epsilon_{\text{intra}}=0.0052$.

taken the same as in Fig. 2. From this figure, we can see that R decreases to a minimal value when p approximately increases to 0.045 at first. Then, with p increasing from 0.045, R increases and reaches a local maximum, marked as C in the figure. Moreover, with p increasing further, R increases again after reaching another point D. The five points A–E labeled in Fig. 3 correspond to the spatiotemporal patterns shown by Figs. 2(a)–2(e), respectively. Therefore, using the order parameter R, burst synchronization transitions from Figs. 2(a) to 2(c) and from Figs. 2(c) to 2(e) have been clearly displayed.

Next, we take the probability $p=0.075$, $\epsilon_{\text{intra}}=0.0052$, and choose the intercoupling strength ϵ_{inter} as control parameter. The spatiotemporal patterns for different values of ϵ_{inter} are depicted in Fig. 4. As shown in Fig. 4(a), the spatiotemporal pattern for $\epsilon_{\text{inter}}=0.002$ is burst synchronized. Its synchrony is destroyed when ϵ_{inter} increases to 0.005 [Fig. 4(b)]. A burst synchronous pattern emerges again when $\epsilon_{\text{inter}}=0.007$, see Fig. 4(c). With further increasing of ϵ_{inter}, the burst synchronous pattern shown in Fig. 4(c) transfers to another burst synchronous one [Fig. 4(e)] via a transition pattern [Fig. 4(d)]. Thus, transitions of burst synchronization can also be induced by the intercoupling strength ϵ_{inter}, as quantitatively characterized by the variation of the order parameter R with respect to ϵ_{inter} exhibited in Fig. 5.

Finally, we fix $p=0.045$, $\epsilon_{\text{inter}}=0.008$, and take the intracoupling strength ϵ_{intra} as control parameter. The numerically obtained spatiotemporal patterns for various ϵ_{intra} are exhibited in Fig. 6, and a variation of the order parameter R vs ϵ_{intra} corresponding to Fig. 6 is presented in Fig. 7. As we see, the obtained results shown in Figs. 6 and 7 together indicate the occurrence of burst synchronization transitions, which are induced by the intracoupling strength.

In order to generalize the above obtained results, we plot the value of R in a two-dimensional parameter space, as shown in Fig. 8. Figure 8(a) exhibits the dependence of R on the intercoupling strength ϵ_{inter} and the probability p with the intracoupling strength $\epsilon_{\text{intra}}=0.0052$. While Fig. 8(b) shows the dependence of R on the intercoupling strength ϵ_{inter} and the intracoupling strength ϵ_{intra} with the probability $p=0.045$. Combined with the above analysis, we can see that burst synchronization transitions are induced by the probability p and the inter- and intracoupling strengths, ϵ_{inter} and ϵ_{intra}, in much wider parameter regions.

B. Burst synchronization transition in a network of subnetworks with $M > 2$

In this subsection, we aim to extend the obtained results to a neuronal network, which contains more than two subnetworks, say $M=5$. Variations of the order parameter R with respect to p, ϵ_{inter}, and ϵ_{intra} are shown in Fig. 9, where $M=5$. From this figure, we can see that the probability p, the inter- and intracoupling strengths ϵ_{inter} and ϵ_{intra} can also induce two burst synchronization transitions in such neuronal networks.

Finally, we study the effect of the number of subnetworks on the transition of burst synchronization when the network size is fixed. We set the inter- and intracoupling strengths as $\epsilon_{\text{inter}}=0.008$, $\epsilon_{\text{intra}}=0.0052$, and the probability $p=0.17$. We consider all the possible values of the

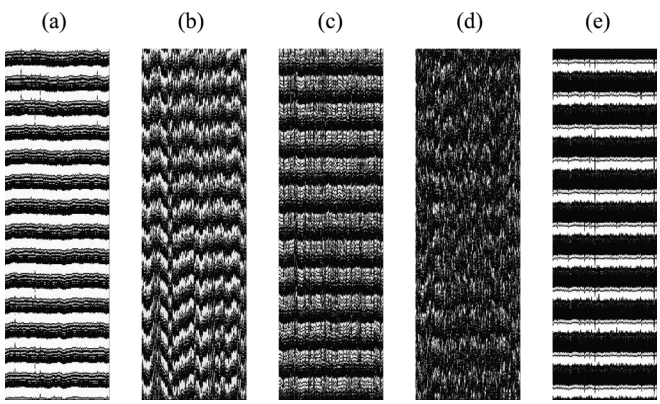

FIG. 4. Two burst synchronization transitions are induced by the intercoupling strength ϵ_{inter}. The spatiotemporal patterns shown in (a) $\epsilon_{\text{inter}}=0.002$, (c) $\epsilon_{\text{inter}}=0.007$, and (e) $\epsilon_{\text{inter}}=0.025$ are burst synchronized patterns, while the spatiotemporal patterns shown in (b) $\epsilon_{\text{inter}}=0.005$ and (d) $\epsilon_{\text{inter}}=0.009$ are the transition ones. Here $N=240$, $M=2$, and $\epsilon_{\text{intra}}=0.0052$, $p=0.075$.

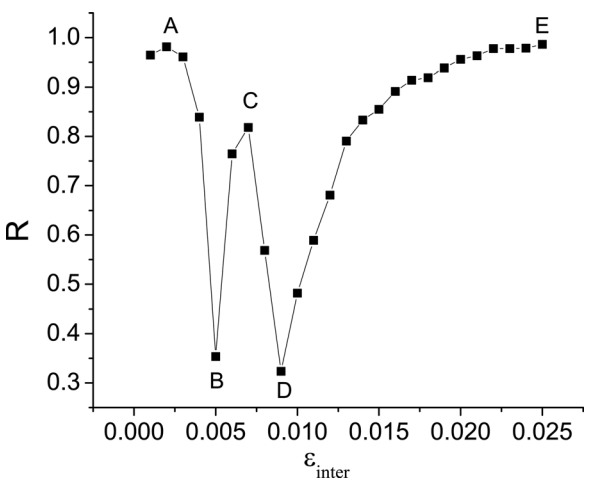

FIG. 5. Variation of the order parameter R with respect to ϵ_{inter} for $p=0.075$ and $\epsilon_{\text{intra}}=0.0052$.

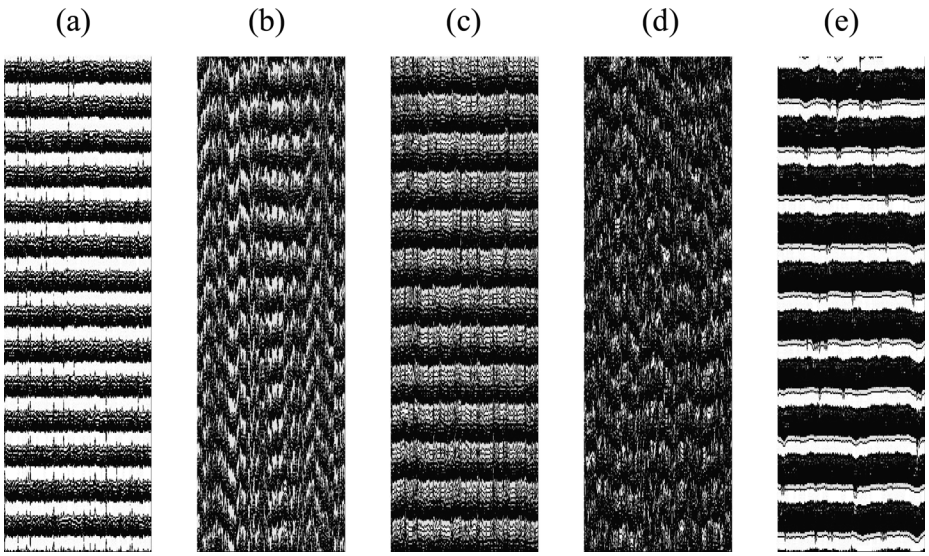

FIG. 6. Two burst synchronization transitions are induced by the intracoupling strength ϵ_{intra}. The spatiotemporal patterns shown in (a) $\epsilon_{\text{intra}}=0.0018$, (c) $\epsilon_{\text{intra}}=0.0072$, and (e) $\epsilon_{\text{intra}}=0.019$ are burst synchronized patterns, while the spatiotemporal patterns shown in (b) $\epsilon_{\text{intra}}=0.0054$ and (d) $\epsilon_{\text{intra}}=0.0096$ are the transition ones. Here $N=240, M=2$, and $\epsilon_{\text{inter}}=0.008, p=0.045$.

subnetwork number M (note that the network size N is fixed to 240). Variation of the order parameter R with respect to all possible values of M is plotted in Fig. 10. The spatiotemporal patterns, corresponding to the marks A, B, C, D, E labeled in Fig. 10, are depicted in Fig. 11. The results exhibited by these two figures indicate that number of subnetworks in a fixed size network can also induce transitions of burst synchronization.

The results obtained for $M>2$ indicate that, except for the intercoupling strength, intracoupling strength, and the probability of random links between different subnetworks, the number of subnetworks can also elicit transitions of burst synchronization.

C. Mechanisms of burst synchronization transitions

With the above observed phenomena, we can conclude that the probability p, the inter- and intracoupling strengths $\epsilon_{\text{inter}}, \epsilon_{\text{intra}}$, and the number of subnetworks are all able to induce burst synchronization transitions in a neuronal network, which contains several subnetworks. However, what is the underlining mechanism of the observed burst synchronization transition? In order to answer this question, we turn back to the first equation of Eqs. (1) and rewrite it as

$$\begin{aligned}\dot{x}_{I,i} &= y_{I,i} - a x_{I,i}^3 + b x_{I,i}^2 - z_{I,i} + I_{\text{ext}} \\ &\quad - (2k\epsilon_{\text{intra}} + \epsilon_{\text{inter}} pn) x_{I,i} \\ &\quad + \epsilon_{\text{intra}} \sum_j A_I(i,j) x_{I,j} + \epsilon_{\text{inter}} \sum_J \sum_j B_{I,J}(i,j) x_{J,j}. \end{aligned} \tag{4}$$

We find that, within the current considered parameter regions, values of the last item $\epsilon_{\text{intra}} \sum_j A_I(i,j)x_{I,j} + \epsilon_{\text{inter}} \sum_J \sum_j B_{I,J}(i,j)x_{J,j}$ in Eq. (4) are mostly near zero for all

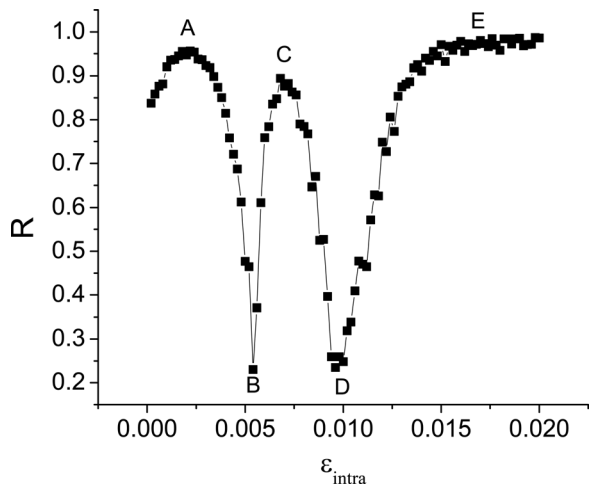

FIG. 7. Variation of the order parameter R with respect to ϵ_{intra} for $p=0.045$ and $\epsilon_{\text{inter}}=0.008$.

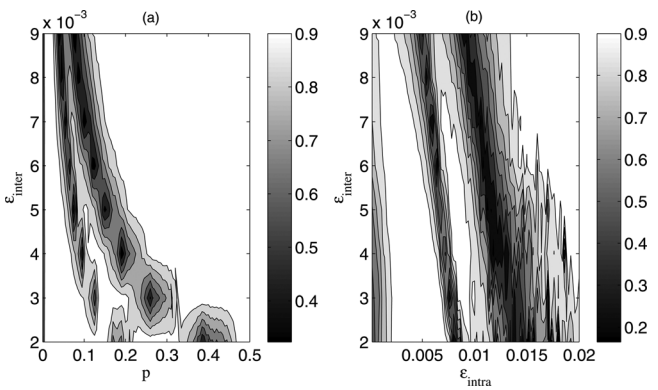

FIG. 8. Dependence of the order parameter R on (a) ϵ_{inter} and p with $\epsilon_{\text{intra}}=0.0052$, and (b) ϵ_{inter} and ϵ_{intra} with $p=0.045$. Burst synchronization transitions induced by the intra- and intercoupling strengths $\epsilon_{\text{intra}}, \epsilon_{\text{inter}}$ and the probability p are clearly visible from these two figures.

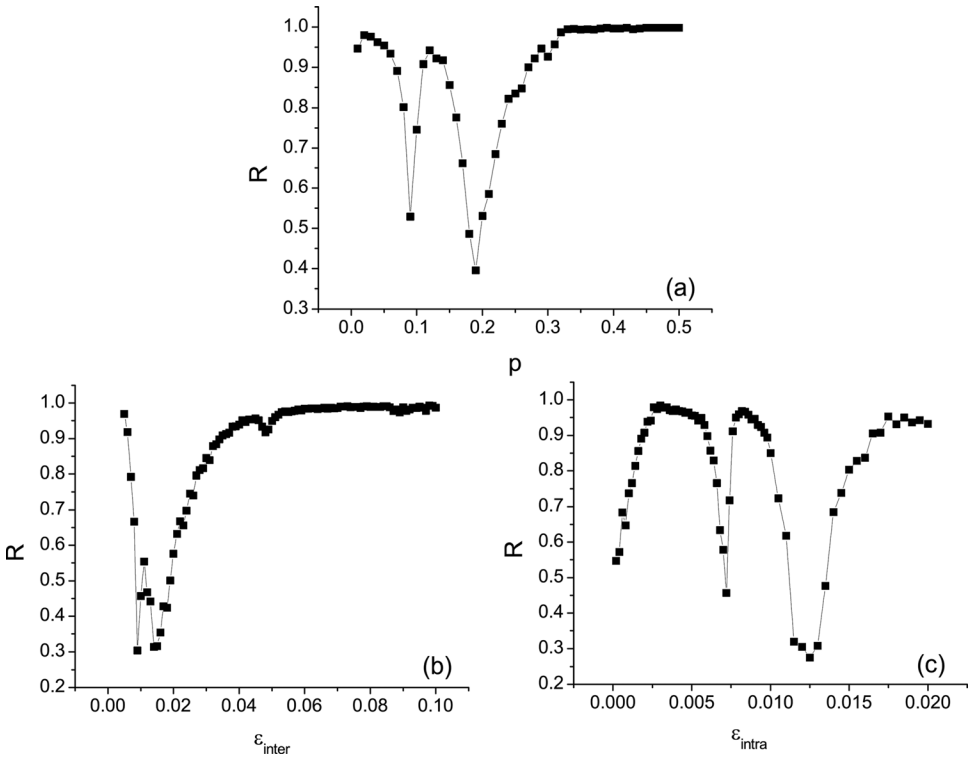

FIG. 9. Variation of the order parameter R with respect to (a) p for $\epsilon_{intra} = \epsilon_{inter} = 0.0052$; (b) ϵ_{inter} for $\epsilon_{intra} = 0.0052$, $p = 0.05$; and (c) ϵ_{intra} for $\epsilon_{inter} = 0.0052$, $p = 0.05$. The network size is $N = 240$ and the number of subnetworks is $M = 5$.

pairs of (I, i). So, this item can be ignored, and Eq. (4) can be approximately written as

$$\dot{x}_{I,i} \approx y_{I,i} - ax_{I,i}^3 + bx_{I,i}^2 - z_{I,i} + I_{\text{ext}} - (2k\epsilon_{\text{intra}} + 2\epsilon_{\text{inter}}pn)x_{I,i}. \tag{5}$$

Before revealing the mechanism of the observed burst synchronization transition, we introduce some results about a single HR neuron ($\dot{x} = y - ax^3 + bx^2 - z + I_{\text{ext}}, \dot{y} = c - dx^2 - y, \dot{z} = r[s(x - x_0) - z]$). Using fast–slow analysis, Shen *et al.*[52] depicted the bifurcation geometry of the fast subsystem ($\dot{x} = y - ax^3 + bx^2 - z + I_{\text{ext}}, \dot{y} = c - dx^2 - y$) by choosing the slow variable z as a control parameter (with values of system parameters taken the same as in this paper), cf. Fig. 2(d) of Ref. 52. From their analysis, it is found that there exist two homoclinic points Z_{hc1} and Z_{hc2}, and a single HR neuron in Eq. (1) exhibits fold-homoclinic (FHC) bursting activities when it is isolated. Moreover, it is found that the two homoclinic points Z_{hc1} and Z_{hc2} could move toward each other under some perturbations, such that both points still remain separated but become closer or collide. Close movement makes the number of spikes per burst increase, while collision elicits the bursting type changing from FHC bursting to fold-Hopf (FH) bursting.[52] As indicated in Ref. 52, a perturbation $\alpha x_{I,i}$ ($\alpha = 2k\epsilon_{\text{intra}} + 2\epsilon_{\text{inter}}pn$) in Eq. (5) can play the role making Z_{hc1} and Z_{hc2} move toward each other. Thus, we

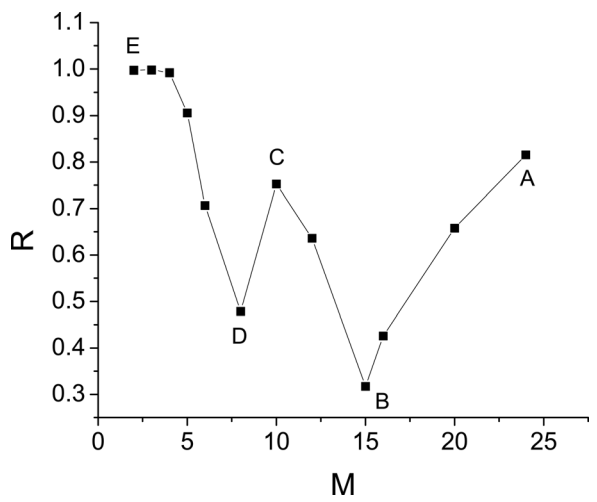

FIG. 10. Variation of the order parameter R with respect to M for $N = 240$, where $\epsilon_{\text{inter}} = 0.008$, $\epsilon_{\text{intra}} = 0.0052$, and $p = 0.17$.

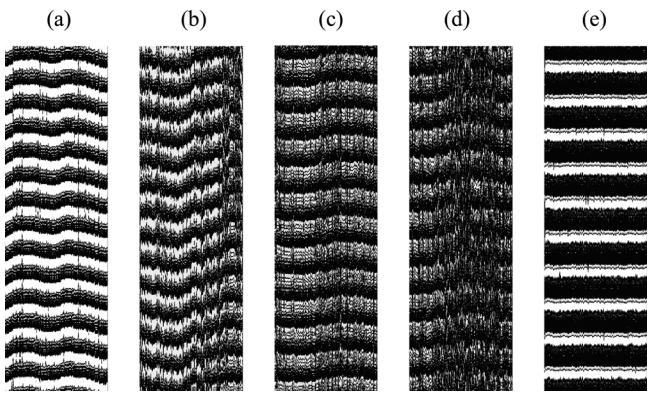

FIG. 11. Two burst synchronization transitions are induced by the number of subnetworks M. The spatiotemporal patterns shown by (a) $M = 24$, (c) $M = 10$, and (e) $M = 2$ are burst synchronized patterns, while the spatiotemporal patterns shown by (b) $M = 15$ and (d) $M = 8$ are the transition ones. Here $N = 240$, and $\epsilon_{\text{inter}} = 0.008$, $\epsilon_{\text{intra}} = 0.0052$, and $p = 0.17$.

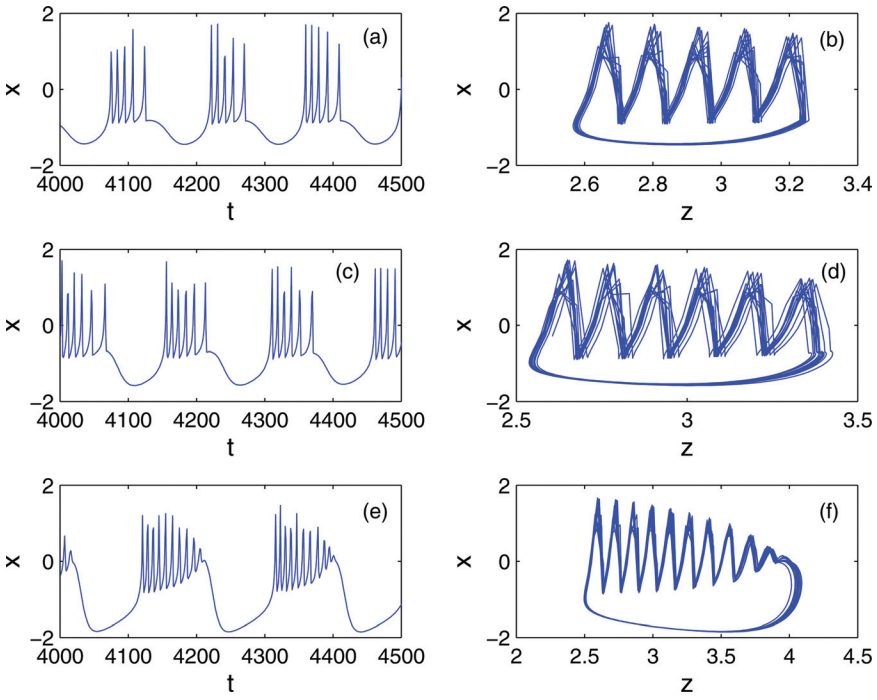

FIG. 12. (Color online) (Left panels) Time series of membrane potential for one typical neuron with (a) $p=0.015$, (c) $p=0.065$, and (e) $p=0.17$, respectively. (Right panels) The corresponding trajectories of the left panels for a randomly chosen neuron. The other parameters are taken the same as in Fig. 2.

speculate that the two burst synchronization transitions observed here may be caused by spike-adding and changes of bursting type, respectively.

In order to test this hypothesis, we plot the spiking time series and phase trajectories of a randomly chosen neuron from the studied system [Eq. (1)] at three burst synchronization states. Here, we take patterns shown in Figs. 2(a), 2(c), and 2(e) as examples. The corresponding spiking time series and phase trajectories are depicted in Fig. 12. From Fig. 12, it can be clearly seen that the spike number in each burst increases from five to six with the bursting type unchanged as p increases from 0.015 to 0.065 [see Figs. 12(a)–12(d)]; and the bursting type changes from FHC to FH bursting with further increasing of p from 0.065 to 0.17 [see Figs. 12(c)–12(f)]. Therefore, the mechanisms of the two observed burst synchronization transitions are clarified: (i) the first burst synchronization transition [i.e., the transition from Fig. 2(a) to 2(c)] occurs via spike-adding; (ii) the second burst synchronization transition [i.e., the transition from Fig. 2(c) to 2(e)] occurs via changes of bursting type from FHC to FH bursting.

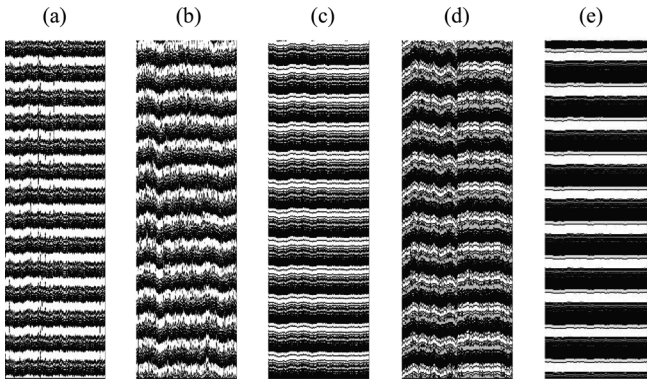

FIG. 13. Burst synchronization transitions are induced by the intracoupling strength in a chemically coupled neuronal network with $M=2$. Burst synchronization patterns transferring from (a) $\epsilon_{\text{intra}}=0.001$ to (c) $\epsilon_{\text{intra}}=0.01$ is via spike-adding, while burst synchronization patterns transferring form (c) $\epsilon_{\text{intra}}=0.01$ to (e) $\epsilon_{\text{intra}}=0.02$ is via change of bursting type. The spatiotemporal patterns shown by (b) $\epsilon_{\text{intra}}=0.005$ and (d) $\epsilon_{\text{intra}}=0.013$ are transition ones. Here $N=240$, and $\epsilon_{\text{inter}}=0.001, p=0.045$.

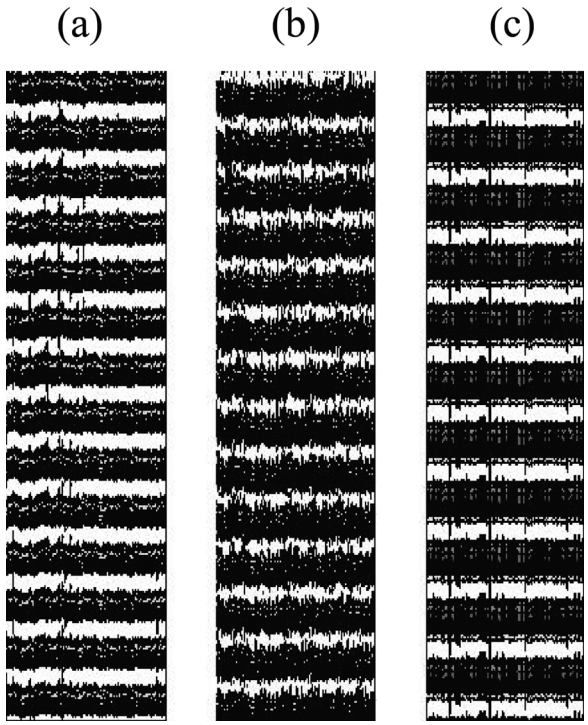

FIG. 14. Burst synchronization transition is induced by the intercoupling strength in a chemically coupled neuronal network with $M=2$. (a) $\epsilon_{\text{inter}}=0.001$, (b) $\epsilon_{\text{inter}}=0.03$, and (c) $\epsilon_{\text{inter}}=0.08$. This burst synchronization transition happens through the change of bursting type. Here $N=240$, and $\epsilon_{\text{intra}}=0.001$, $p=0.045$.

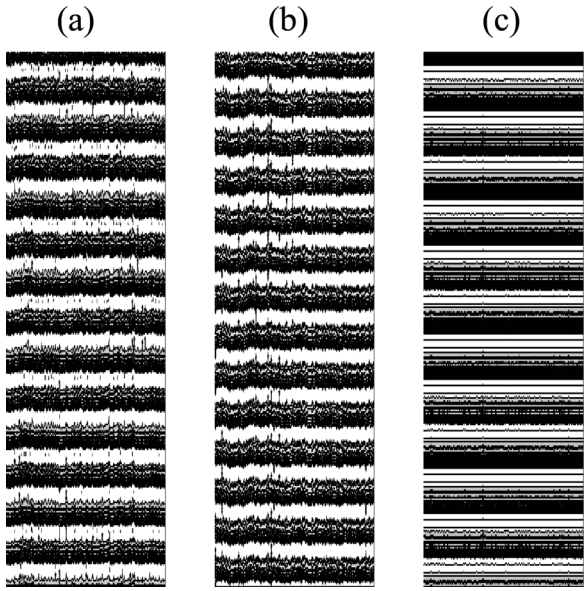

FIG. 15. Burst synchronization transition is induced by p in a chemically coupled neuronal network with $M=2$. (a) $p=0.045$, (b) $p=0.3$, and (c) $p=0.5$. This burst synchronization transition happens through the change of spiking number per burst. Here $N=240$, and $\epsilon_{\text{intra}}=\epsilon_{\text{inter}}=0.001$.

IV. DISCUSSION

In the present work, we have only considered the neuronal network with electrical couplings. Thus, what happens if the neuronal network is coupled with chemical synapses? In order to study this, we replace the first equation of Eqs. (1) by

$$\begin{aligned}\dot{x}_{I,i} &= y_{I,i} - ax_{I,i}^3 + bx_{I,i}^2 - z_{I,i} + I_{\text{ext}} + \epsilon_{\text{intra}} \\ &\times (V_s - x_{I,i}) \sum_j A_I(i,j)\Theta(x_{I,j}) + \epsilon_{\text{inter}}(V_s - x_{I,i}) \\ &\times \sum_J \sum_j B_{I,J}(i,j)\Theta(x_{J,j}). \end{aligned} \tag{6}$$

Then, Eq. (1) is changed to

$$\begin{aligned}\dot{x}_{I,i} &= y_{I,i} - ax_{I,i}^3 + bx_{I,i}^2 - z_{I,i} + I_{\text{ext}} + \epsilon_{\text{intra}} \\ &\times (V_s - x_{I,i}) \sum_j A_I(i,j)\Theta(x_{I,j}) + \epsilon_{\text{inter}}(V_s - x_{I,i}) \\ &\times \sum_J \sum_j B_{I,J}(i,j)\Theta(x_{J,j}), \\ \dot{y}_{I,i} &= c - dx_{I,i}^2 - y_{I,i}, \\ \dot{z}_{I,i} &= r[s(x_{I,i} - x_0) - z_{I,i}], \end{aligned} \tag{7}$$

where V_s is the reversal potential and $\Theta(x)$ is the Heaviside function, which is 1 for $x > \Theta_s$ and 0 otherwise. Here V_s and Θ are taken as 0.0 and -1.0, respectively. The simulation results of Eqs. (7) are shown by Figs. 13–17. We can see that the two burst synchronization transitions observed in electrically coupled case can only be induced by the intracoupling strength. Nonetheless, the other factors, e.g., the intercoupling strength and the probability for random links between different subnetworks, can also induce one of them. For example, the intercoupling strength ϵ_{inter} can induce burst synchronization transition by changing from FHC to FH bursting [see Figs. 14 and Figs. 17(a) and 17(b)], and the probability for random links between different subnetworks p can induce burst synchronization transition through the change of spiking number per burst [see Figs. 15 and 17(c) and 17(d)].

Additionally, the present results are based on the simulation of network dynamics with HR neurons set. In order to see whether the results (the two burst synchronization transitions when varying topological properties of the network) reproduced using other models of bursting dynamics for the nodes, we applied Morris–Lecar[59] and Chay[60] models. But unfortunately, we do not observed similar results. Therefore, the obtained results in this paper are the interplay between network topology and the individual dynamics. They not only depend on the properties of the network topology but also on the intrinsic properties of each individual dynamical system.

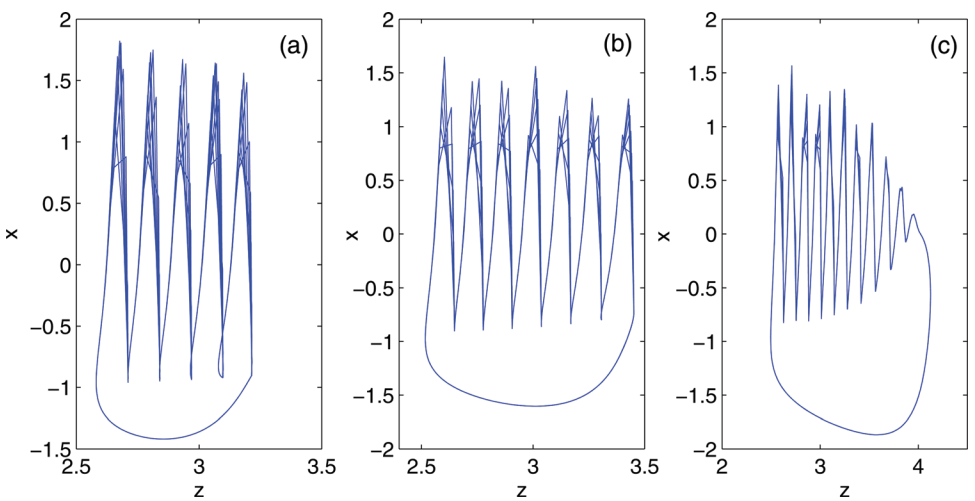

FIG. 16. (Color online) Phase portraits of a single neuron for chemical synapses. From (a) to (c), $\epsilon_{\text{intra}}=0.001$, 0.01, and 0.02, respectively. Spike-adding and transition to FH bursting are both observed. Here $N=240$, and $\epsilon_{\text{intra}}=0.001$, $p=0.045$.

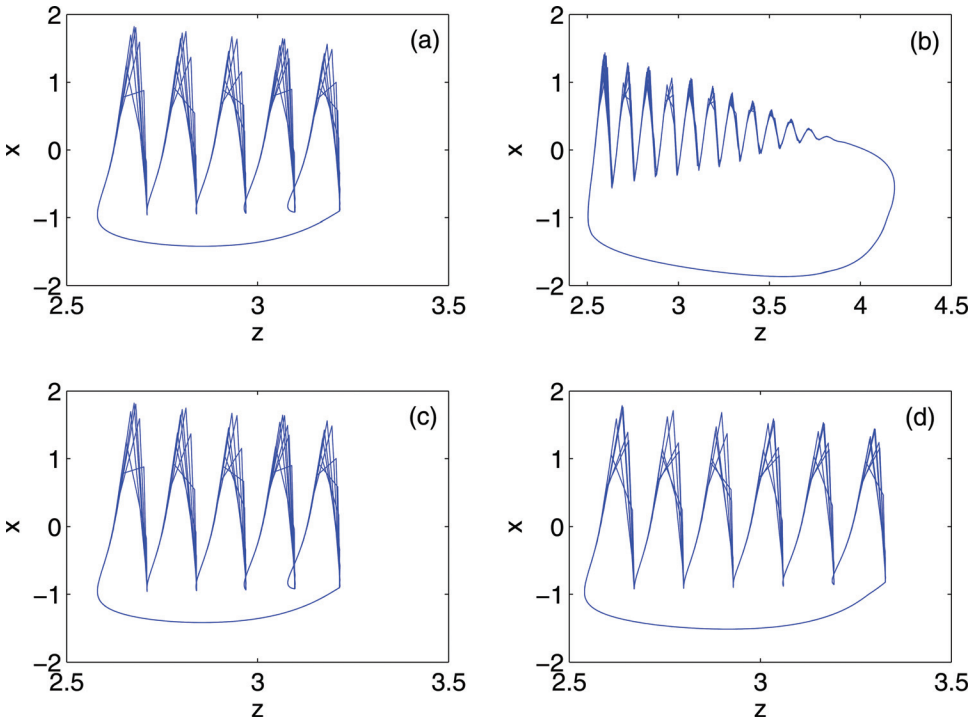

FIG. 17. (Color online) Phase portraits of a single neuron for chemical synapses. (i) Transition from FHC bursting to FH bursting is observed as ϵ_{inter} increasing from (a) $\epsilon_{inter}=0.001$ to (b) $\epsilon_{inter}=0.08$, where $N=240$, $\epsilon_{intra}=0.001$, and $p=0.045$. (ii) Spike-adding is observed as p increases from (c) $p=0.045$ to (d) $p=0.5$, where $N=240$, and $\epsilon_{inter}=\epsilon_{intra}=0.001$.

V. CONCLUSIONS

In this paper, we mainly study burst synchronization transitions in an electrically coupled neuronal network, which consists of several subnetworks. With the obtained numerical results, we show that several factors—the intra- and intercoupling strength, the probability for random links between different subnetworks and the number of subnetworks—can induce transitions between different burst synchronized states. In this paper, we have observed two types of burst synchronization transitions. We have shown that the underlining mechanisms of the observed burst synchronization transitions are different: one is via spike-adding and the other one is via a change of bursting type.

The brain's plasticity refers to the brain's ability to change its structure and function during maturation, learning, environmental challenges, or pathology. Brain plasticity is expressed by modifying the strength or efficacy of synaptic transmission at preexisting synapses, eliciting the growth of new synaptic connections or the pruning away of existing ones, or modulating the excitability properties of individual neurons.[61] In this paper, we study the effects of coupling strength (intra- and intercoupling strength), number of connections (probability of random links between different subnetworks and number of subnetworks) on burst synchronization of a neuronal network. Thus, our obtained results might also give significant implications on the role of brain plasticity in some functional behavior associated with synchronization.

ACKNOWLEDGMENTS

This work was supported by the National Natural Science Foundation of China (Grant Nos. 10872014 and 10972018). Xiaojuan Sun is thankful for the support from the China Postdoctoral Science Foundation Project (Grant No. 20090460337), Matjaž Perc acknowledges support from the Slovenian Research Agency (Grant No. Z1-2032), Jürgen Kurths acknowledges support from the BMBF (BCCN) and EU (PHOCUS), and Guanrong Chen acknowledges support from the Hong Kong Research Grants Council (Grant No. CityU 117/10E).

APPENDIX: DEFINITIONS OF FHC AND FH BURSTING

The bursting is said to be of the (FHC) type if the resting state disappears via a saddle-node (fold) bifurcation and the spiking limit cycle disappears via saddle homoclinic orbit bifurcation.[62]

The bursting is said to be of the (FH) type if the stable equilibrium corresponding to the resting state disappears via saddle-node (fold) bifurcation and the limit cycle attractor corresponding to the spiking state shrinks to a point via supercritical Andronov-Hopf bifurcation.[62]

[1]M. Barahona and L. Pecora, Phys. Rev. Lett. **89**, 054101 (2002).
[2]X. Wang and G. Chen, Int. J. Bifurcation Chaos Appl. Sci. Eng. **12**, 187 (2002).
[3]T. Nishikawa, A. Motter, Y. Lai, and F. Hoppensteadt, Phys. Rev. Lett. **91**, 014101 (2003).
[4]A. Motter, C. Zhou, and J. Kurths, Europhys. Lett. **69**, 334 (2005).
[5]C. Zhou and J. Kurths, Phys. Rev. Lett. **96**, 164102 (2006).
[6]A. Arenas, A. D'iaz-Guilera, and C. Pérez-Vicente, Physica D **224**, 27 (2006).
[7]J. Gómez-Gardeñes, Y. Moreno, and A. Arenas, Phys. Rev. Lett. **98**, 034101 (2007).
[8]Y. Hung, Y. Huang, M. Ho, and C. Hu, Phys. Rev. E **77**, 016202 (2008).
[9]A. Arenas, A. D'iaz-Guilera, J. Kurths, Y. Moreno, and C. Zhou, Phys. Rep. **469**, 93 (2008).
[10]K. Park, Y. Lai, S. Gupte, and J. Kim, Chaos **16**, 015105 (2006).

[11]L. Huang, K. Park, Y. Lai, L. Yang, and K. Yang, Phys. Rev. Lett. **97**, 164101 (2006).
[12]T. Zhou, M. Zhao, G. Chen, G. Yan, and B. Wang, Phys. Lett. A **368**, 431 (2007).
[13]L. Huang, Y. Lai, and R. Gatenby, Phys. Rev. E **77**, 016103 (2008).
[14]S. Guan, X. Wang, Y. Lai, and C. Lai, Phys. Rev. E **77**, 016103 (2008).
[15]Y. Fujiwara-Tsukamoto, Y. Isomura, A. Nambu, and M. Takada, Neurosci. **119**, 265 (2003).
[16]S. Neuenschwander, M. Castelo-Branco, and W. Singer, Vision Res. **39**, 2485 (1999).
[17]C. Gray, A. Engel, P. König, and W. Singer, Visual Neurosci. **8**, 337 (1992).
[18]R. Traub and R. Wong, Science **216**, 745 (1982).
[19]C. Babiloni, R. Ferri, D. V. Moretti, A. Stramb, G. Binetti, G. D. Forno, F. Ferreri, B. Lanuzza, C. Bonato, F. Nobili, G. Rodriguez, S. Salinari, S. Passero, R. Rocchi, C. J. Stam, and P. M. Rossini, Eur. J. Neurosci. **19**, 2583 (2004).
[20]A. Schnitzler and J. Gross, Nat. Rev. Neurosci. **6**, 285 (2005).
[21]A. Riehle, S. Grün, M. Diesmann, and A. Aertsen, Science **278**, 1950 (1997).
[22]P. Steinmetz, A. Roy, P. Fitzgerald, S. Hsiao, K. Johnson, and E. Niebur, Nature (London) **404**, 187 (2000).
[23]P. Fries, P. Roelfsema, A. Engel, P. König, and W. Singer, Proc. Natl. Acad. Sci. U.S.A. **94**, 12699 (1997).
[24]C. Hilgetag and M. Kaiser, Neuroinformatics **2**, 353 (2004).
[25]O. Sporns, D. Chialvo, M. Kaiser, and C. Hilgetag, Trends Cogn. Sci. **8**, 418 (2004).
[26]C. Zhou, L. Zemanová, G. Zamora-López, C. Hilgetag, and J. Kurths, New J. Phys. **9**, 178 (2007).
[27]N. Malik, B. Ashok, and J. Balakrishnan, Eur. Phys. J. B **74**, 177 (2010).
[28]Q. Wang, Z. Duan, L. Huang, G. Chen, and Q. Lu, New J. Phys. **9**, 383 (2007).
[29]E. Izhikevich, SIAM Rev. **43**, 315 (2001).
[30]J. Shuai and D. Durand, Phys. Lett. A **264**, 289 (1999).
[31]Y. Gong, M. Wang, Z. Hou, and H. Xin, ChemPhysChem **6**, 1042 (2005).
[32]C. Zhou and J. Kurths, Phys. Rev. Lett. **88**, 230602 (2002).
[33]J. Wang, B. Deng, and X. Fei, Chaos, Solitons Fractals **35**, 512 (2008).
[34]Y. Sato and M. Shiino, Phys. Rev. E **75**, 011909 (2007).
[35]M. Perc, Biophys. Chem. **141**, 175 (2009).
[36]M. Yoshioka, Phys. Rev. E **71**, 065203 (2005).
[37]H. Hasegawa, Phys. Rev. E **72**, 056139 (2005).
[38]R. Krahe and F. Gabbiani, Nature Rev. Neurosci. **5**, 13 (2004).
[39]C. Vreeswijk and D. Hansel, Neural Comput. **13**, 959 (2001).
[40]M. Dhamala, V. Jirsa, and M. Ding, Phys. Rev. Lett. **92**, 028101 (2004).
[41]M. Ivanchenko, G. Osipov, V. Shalfeev, and J. Kurths, Phys. Rev. Lett. **93**, 134101 (2004).
[42]T. Pereira, M. Baptista, and J. Kurths, Eur. Phys. J. Spec. Top. **146**, 155 (2007).
[43]I. Belykh, E. Lange, and M. Hasler, Phys. Rev. Lett. **94**, 188101 (2005).
[44]I. Belykh, and A. Shilnikov, Phys. Rev. Lett. **101**, 078102 (2008).
[45]X. Shi and Q. Lu, Physica A **388**, 2410 (2009).
[46]M. Dhamala, K. Viktor, and M. Ding, Phys. Rev. Lett. **92**, 074104 (2004).
[47]N. Burić, K. Todorovć, and N. Vasović, Phys. Rev. E **78**, 036211 (2008).
[48]N. Burić, K. Todorovć, and N. Vasović, Phys. Rev. E **75**, 067204 (2007).
[49]C. Batista, A. Batista, J. Pontes, S. Lopes, and R. Viana, Chaos, Solitons Fractals **41**, 2220 (2009).
[50]J. Pontes, R. Viana, S. Lopes, C. Batista, and A. Batista, Physica A **387**, 4417 (2008).
[51]N. Rulkov, Phys. Rev. Lett. **86**, 183 (2001).
[52]Y. Shen, Z. Hou, and H. Xin, Phys. Rev. E **77**, 031920 (2008).
[53]Q. Wang, Z. Duan, Z. Feng, G. Chen, and Q. Lu, Physica A **387**, 4404 (2008).
[54]X. Liang, M. Tang, M. Dhamala, and Z. Hou, Phys. Rev. E **80**, 066202 (2009).
[55]Q. Wang, Q. Lu, and G. Chen, Physica A **374**, 869 (2007).
[56]Q. Wang, Q. Lu, and G. Chen, Int. J. Bifurcation Chaos Appl. Sci. Eng. **18**, 1189 (2008).
[57]J. Hindmarsh and R. Rose, Proc. R. Soc. London, Ser. B **221**, 87 (1984).
[58]M. Ivanchenko, G. Osipov, V. Shalfeev, and J. Kurths, Phys. Rev. Lett. **98**, 108101 (2007).
[59]C. Morris and H. Lecar, Biophys. J. **35**, 193 (1981).
[60]T. Chay, Physica D **16**, 233 (1985).
[61]K. Davis, D. Charney, J. Coyle, and C. Nemeroff, *Neuropsychopharmacology: The Fifth Generation of Progress* (Lippincott Williams and Wilkins, Philadelphia, 2002).
[62]E. Izhikevich, *Dynamical Systems in Neuroscience: The Geometry of Excitability and Bursting* (The MIT Press, Cambridge, 2007).